DOI: 10.48011/sbse.v1i1.2229

Simulation of a Superconductor Fault Current Limiter with finite element method using A-V-H formulation

G. d. Santos*. F.G.R. Martins. * B.M.O Santos D.H.N.Dias.***
F. Sass. *G.G. Sotelo*

Universidade Federal Fluminense
Universidade Federal do Rio de Janeiro
BR (e-mail: dosgabrielsantos@poli.ufrj.br).
** Electrical Engineering Department, Universidade Federal Fluminense,*
*** Electrical Engineering Department, Universidade Federal do Rio de Janeiro.*

Abstract: Nowadays, the complexity of electrical power systems is increasing. Consequently, the occurrence and the amplitude of the fault current are rising. This fault currents harm the substations' electrical equipment. Besides, the growth in the fault current level is forcing the change of the circuit breakers to others with a higher interruption capability. A proposal to solve this problem is the fault current limiter (FCL). This equipment has low impedance in the normal operation and high impedance in a short circuit moment. Superconductors are an advantageous choice of material in this case, because of their properties. In order to simulate this equipment, the 2-D Finite Element Method (FEM) has been used. In this paper, a novel FEM simulation analysis of the saturated core Superconductor Fault Current Limiter (SFCL) is proposed using the A-V-H formulation. The current distribution in the superconducting coil is observed. The results are compared to the limited fault current measurements and simulations available in the literature.

Keywords: Superconducting Fault Current Limiting (SFCL), Saturated Core Fault Current Limiting, Short Circuit, Finite Element Method, A-V formulation, H-formulation.

1. INTRODUCTION

Over the years, the power demand has been growing to attend the needs of the countries and continents ("World Energy Outlook 2019 – Analysis," n.d.). Hence, a rise in fault current amplitude and the number of occurrences is observed. Examples of this effect are distributed generation and offshore systems. These examples have the same characteristic, low impedance. Then, the short circuit level for these systems is high, increasing operation cost toe industries (Hasan et al., 2008; Raza et al., 2018).

A proposal to reduce short circuit level is the Superconducting Fault Current Limiter (SFCL) (Hong et al., 2009; Neumueller et al., 2009). In the literature, there are two more common types of SFCL (Dommerque et al., 2010; Elschner et al., 2012, 2011). The first one is called resistive-SFCL and the second one is named such as inductive-SFCL. The inductive SFCL type has two ramifications: the first one named inductive saturated core SFCL, and the second topology called inductive shielded core SFCL (Hekmati, 2014; Morandi et al., 2013). The thermal-electromagnetic models, projects and experimental tests of the shielded core inductive type are presented in (Ferreira et al., 2015; Qiu et al., 2018; Rajabi and Mousavi G., 2019).

The inductive saturated cores SFCL has two iron cores per phase, two ac windings, and a DC bias to saturate the iron cores in normal operation. The conceptual three-phase designing of this equipment is shown in figure 1. The conceptual three-phase design of this equipment is shown in figure 2. It is possible to see in figure 1 that there is one DC bias to the magnetization of all iron cores. The six AC windings are used as a couple per phase. Therefore, there are two AC connections per phase, where the SFCL is connected into the grid, and there are connections for the DC circuit. This equipment was simulated by FEM and electromagnetic circuit in (Vilhena et al., 2015; Wang et al., 2009; Zhang et al., 2011), and it was tested in (Fajoni et al., 2015; Moriconi et al., 2011; Nikulshin et al., 2016).

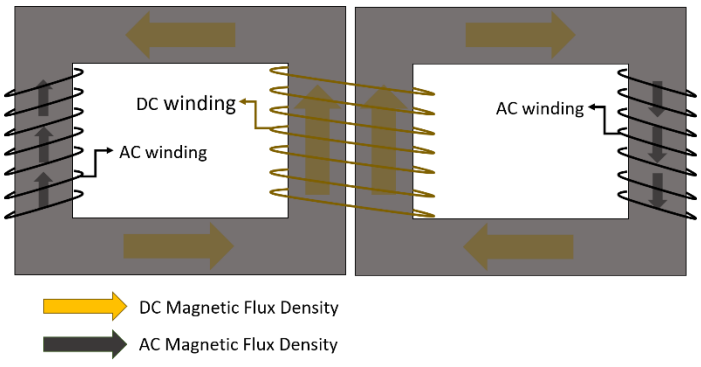

Fig 1 Schematic saturated iron-core inductive SFCL.

The objective of this paper is to analyze a saturated iron core SFCL with bidimensional finite elements using the A-V-H formulation. This novel formulation is joining the A-V with H formulations. The first one has the vector magnetic potential

as the state variable, and it is already implemented in various commercial software.

The second formulation was developed to simulate materials with high non-linearity in the E-J curve, and it has the magnetic field intensity as the state variable. They are coupled using boundary conditions.

The results show the distribution of the current density. The prospective current and the limited short circuit are also presented.

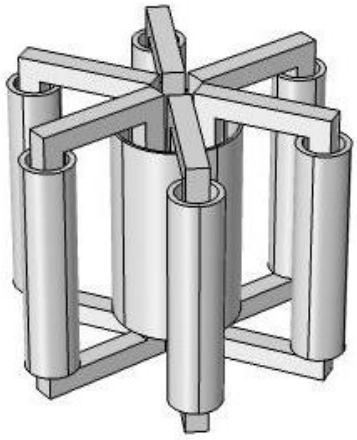

Fig 2 Design of the saturated inductive core SCFL.

2. Methodology

2.1 A-V-H Formulation

This section explains the FEM technique used in this work. In A-V-H, the domains are divided into two regions. Figure 3 demonstrates the division with tramodel line. This boundary divides the regions into normal (simulated by A-formulation) and superconducting (simulated by H-formulations). The region Ω_{sup} contains the superconductor material and it is simulated by H formulation. The $\Omega_{non-sup}$ is the region without superconductor and the applied formulation is A-V. Therefore, it is possible to use non-linear models for ferromagnetic materials. Hence, the model converges fast. Implementation is easy since there are many commercial software that have the A-V formulation ready for use.

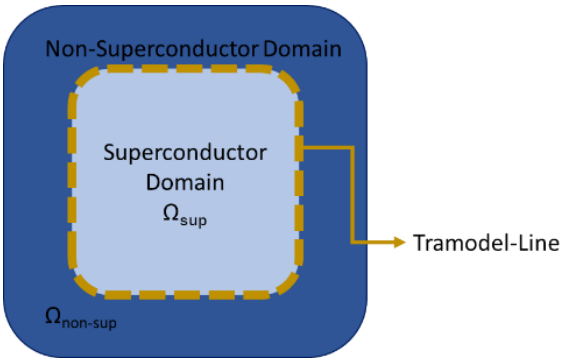

Fig 3 Division of regions in the A-V-H formulation.

The A-V formulation is defined by

$$\sigma(|E|)\frac{\partial \boldsymbol{A}}{\partial t} - \frac{1}{\mu}\nabla^2 \boldsymbol{A} = \boldsymbol{J_e} \quad (1)$$

$$\boldsymbol{B} = \nabla \times \boldsymbol{A} \quad (2)$$

$$\boldsymbol{J} = \sigma(|E|)\boldsymbol{E} + \boldsymbol{J_e} \quad (3)$$

$$\boldsymbol{E} = -\frac{\partial \boldsymbol{A}}{\partial t} \quad (4)$$

where A is the magnetic vector potential, $\sigma(|E|)$ is the electrical conductivity, Je is the external current density, J is the total current density, B is the magnetic flux density, E is the electrical field and μ is the magnetic permeability.

The H-formulation is defined by

$$\mu\frac{\partial \boldsymbol{H}}{\partial t} + \nabla \times \boldsymbol{E} = \boldsymbol{0} \quad (5)$$

$$\boldsymbol{J} = \nabla \times \boldsymbol{H} \quad (6)$$

$$\boldsymbol{E} = \rho(|J|)\boldsymbol{J} \quad (7)$$

$$\rho(|J|) = \frac{E_c}{J_c}\left|\frac{J}{J_c}\right|^{n-1} \quad (8)$$

where $\rho(|J|)$ is the electrical resistivity of the superconductor, Jc is the critical current density, Ec is the critical electrical field (typically $1\frac{\mu V}{cm}$), n is the transition index. To apply current in the superconductor, an integral restriction is used:

$$I_{app} - \int \boldsymbol{J}.d\boldsymbol{S} = 0 \quad (9)$$

The coupling conditions are imposed in the weak form of the finite elements and are given by.

$H_t^H.test(A_z^A)$ – Applied in A-formulation[1] (10)

$E_z^A.test(H_t^H)$ – Applied in H-formulation (11)

In this case, H_t is the source for the A-V formulation and E_z is the source for the 2D H formulation. constructed for the 2D (Brambilla et al., 2018; Dias et al., 2019; Santos, n.d.).

2.2 A-V-H formulation applied in the SFCL problem

The superconducting winding is modeled by the homogenization process (Sass et al., 2015). Therefore, the engineering critical current density is given by equation 12-13:

$$\boldsymbol{J_{cEng}} = \boldsymbol{J_c} \cdot \gamma \quad (12)$$

$$\gamma = \frac{A_{superconductor}}{A_{tape}} \quad (13)$$

where $\boldsymbol{J_{cEng}}$ is the engineering critical current density, $A_{superconductor}$ and A_{tape} are the cross-section area of the superconductor and tape respectively. In this work is used the Anderson-Kim model for modeling the current density's dependence of the magnetic flux density:

$$\boldsymbol{Jc}(|\boldsymbol{B}|) = \frac{\boldsymbol{Jc_0}}{1 + \frac{|B_y|}{\boldsymbol{B0}}} \quad (14)$$

where J_{c0} is the critical current density at self-field in 77K, B_y is the y component of the magnetic flux. B_0 is the parameter obtained from experimental curve.

$\mathbf{J_{c0}}$ is given by the I_{c0} measured during the V-I test after the critical current is divided by height and width of the superconductor. In this article, the B_0 is equal to 0.5 T and the critical current is 250 A.

The 2D-geometry is shown in figure 4, where the left and right rectangles represent the copper winding, and the central rectangle represents the superconducting winding. Figure 4 has a zoom at the superconductor region in order to show the tramodel line. In addition, the air and the iron-core are modeled. The materials properties are summarized in Table 1:

Table 1 Materials properties used at present work

Air	
σ	$1\,S/m$
μ	$4\pi \cdot 10^{-7} H/m$
ρ	$1\frac{\Omega}{m}$
Copper	
σ	$6 \cdot 10^7\,S/m$
μ	$4\pi \cdot 10^{-7} H/m$
ρ	–
Superconductor	
σ	–
μ	$4\pi \cdot 10^{-7} H/m$
ρ	$\frac{Ec}{Jc(\lvert\boldsymbol{B}\rvert)}\left\lvert\frac{\boldsymbol{J}}{Jc(\lvert\boldsymbol{B}\rvert)}\right\rvert^{n-1}\frac{\Omega}{m}$
Iron	
σ	$1\,S/m$
μ	$f(B,H)\,H/m$
ρ	–

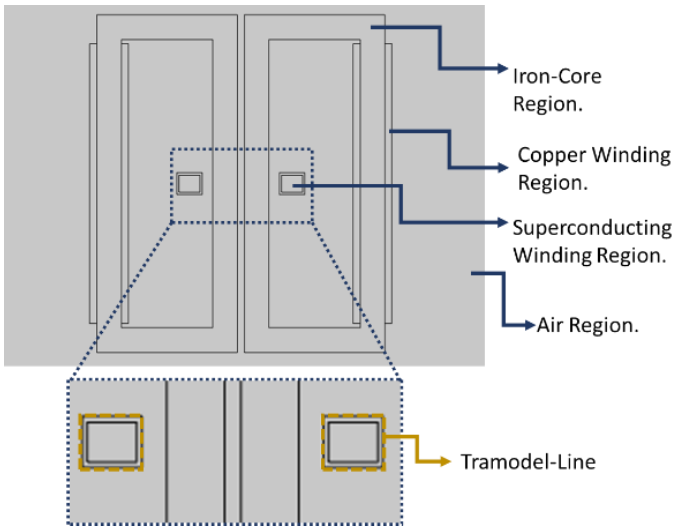

Fig 4 Domain divisions

The B-H hysteresis curve for the ferromagnetic core is modeled by an interpolation function, and is observed in figure 5:

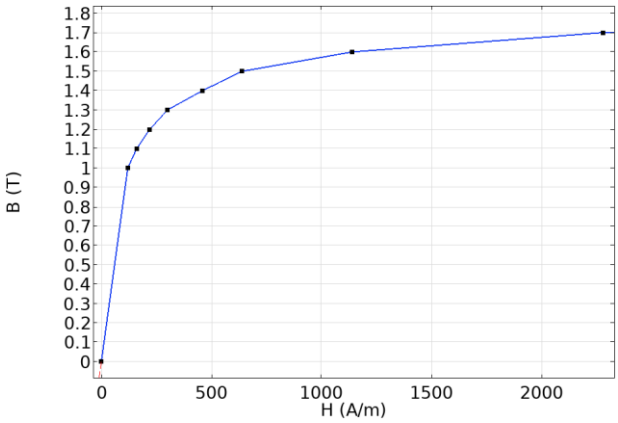

Fig 5 B-H Curve of the ferromagnetic material

The simulations were done in a commercial software COMSOL, where the Magnetic Field physics was used to model the A-V formulation. The H-formulation was implemented by PDE using the General Form PDE.

5. RESULTS

The results are presented and discussed in this section. The mesh used to compute the A-V and H-formulations can be observed in figure 6. The minimum element quality is 0.4868 and the Average element quality is 0.8581.

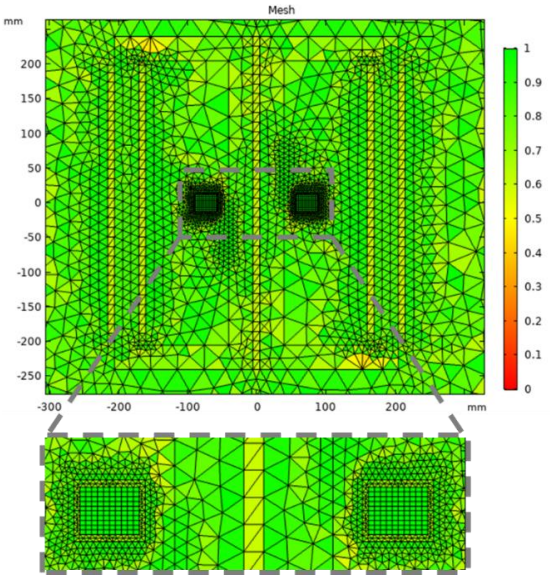

Fig 6 Mesh of the simulation

In figure 7 is possible to see the distribution of the current density normalized by the engineering critical current density inside the superconductor, where the I_{dc} is the direct current applied in the superconductor coil. This behavior follows the Power-Law equation introduced in the above section.

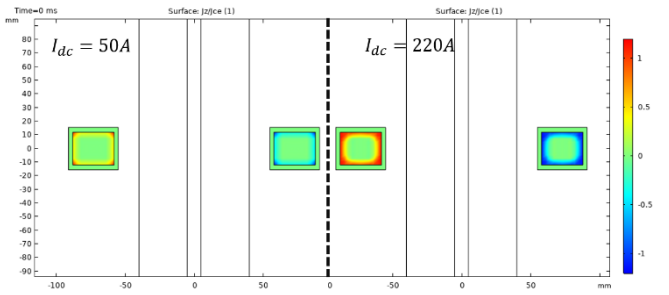

Fig 7 Current density in the superconductor material

Finally, the results of the prospective and limited current are presented in figure 8. The prospective fault current was set in 1.6kA and the normal operating current was 30A, this current is used to simulate the system operating normally. The direct current of the superconductor was varied with these values 50, 60, 70, 140 and 220 A, in order to analyze the effect of the direct current's value in the limitation of the short circuit.

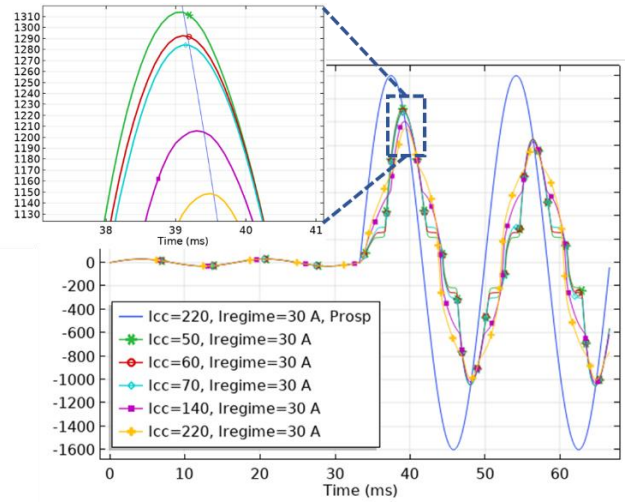

Fig 8 Fault Current Limitation

In figure 8 is possible to see the max limitation is 1140A and it corresponds to 28,75% of the limitation. It is calculated by

$$Limitation = \frac{I_{prospective} - I_{limited}}{I_{prospective}} x\ 100\ (\%) \qquad (15)$$

This simulation result is compared with the real-life test done in (Fajoni et al., 2015). In Fajoni's works, the windings are of the copper and the tests are done for 1.6kA prospective fault current. The maximum value of the limited fault current measured by Fajoni was 1284A and the direct current applied in DC coil in this situation was equal to 70 A. In the simulation, the maximum value calculated is equal to 1285 A. Comparing the Fajoni's result with the simulation results with the same direct current applied in DC coil, the relative error is equal to 0.08%. Hence, it demonstrates the simulation has a good agreement with the results of the real-life test done by Fajoni.

6. CONCLUSION

This work presented a simulation of the inductive saturated core SCFL using finite elements and the A-V-H formulation. The critical current density profile was presented for different direct currents applied. The dependence of the magnetic flux density was implemented in the model of the superconducts critical current density. The future works will study the influence of the leakage magnetic flux density of the core over the superconductor and its critical current density.

This work presented the limitation of the short circuit for five different direct currents applied at the superconductor coil. A comparison of the simulation results with Fajoni's results is done and it presents good quality results when comparing it with real-life tests.

In future works, a 3d version of this simulation will be done. With this model, it will be possible to simulate different short circuits types, such as a three-phase short circuit and a bi-phase short circuit. The 3D model can be implemented with 3D- A-V-H formulation, expanding the formulation developed in (Brambilla et al., 2018) or it can be modeled by 3D T-A formulation (Benkel et al., 2019; Berrospe-Juarez et al., 2018).

ACKNOWLEDGMENT

The acknowledgments are given to CAPES and CNPq for funding this research and its researchers.

REFERENCES

Benkel, T., Lao, M., Liu, Y., Pardo, E., Wolfstädter, S., Reis, T., Grilli, F., 2019. T-A Formulation to Model Electrical Machines with HTS Coated Conductor Coils. ArXiv190102370 Cond-Mat.

Berrospe-Juarez, E., Zermeño, V.M.R., Trillaud, F., Grilli, F., 2018. T-A homogenized and multi-scale models with real-time simulation capabilities for large-scale HTS systems. ArXiv181204414 Phys.

Brambilla, R., Grilli, F., Martini, L., Bocchi, M., Angeli, G., 2018. A Finite-Element Method Framework for Modeling Rotating Machines With Superconducting Windings. IEEE Trans. Appl. Supercond. 28, 1–11. https://doi.org/10.1109/TASC.2018.2812884

Dias, F.J.M., Santos, B.M.O., Sotelo, G.G., Polasek, A., de Andrade, R., 2019. Development of a Superconducting Machine With Stacks of Second Generation HTS Tapes. IEEE Trans. Appl. Supercond. 29, 1–5. https://doi.org/10.1109/TASC.2019.2898252

Dommerque, R., Krämer, S., Hobl, A., Böhm, R., Bludau, M., Bock, J., Klaus, D., Piereder, H., Wilson, A., Krüger, T., Pfeiffer, G., Pfeiffer, K., Elschner, S., 2010. First commercial medium voltage superconducting fault-current limiters: production, test and installation. Supercond. Sci. Technol. 23, 034020. https://doi.org/10.1088/0953-2048/23/3/034020

Elschner, S., Kudymow, A., Brand, J., Fink, S., Goldacker, W., Grilli, F., Noe, M., Vojenciak, M., Hobl, A., Bludau, M., Jänke, C., Krämer, S., Bock, J., 2012. ENSYSTROB – Design, manufacturing and test of a 3-phase resistive fault current limiter based on coated conductors for medium voltage application. Phys. C Supercond. Its Appl., 2011 Centennial superconductivity conference – EUCAS–ISEC–ICMC 482, 98–104. https://doi.org/10.1016/j.physc.2012.04.025

Elschner, S., Kudymow, A., Fink, S., Goldacker, W., Grilli, F., Schacherer, C., Hobl, A., Bock, J., Noe, M., 2011. ENSYSTROB—Resistive Fault Current Limiter Based on Coated Conductors for Medium Voltage Application. IEEE Trans. Appl. Supercond. 21, 1209–1212. https://doi.org/10.1109/TASC.2010.2100799

Fajoni, F., Ruppert, E., Baldan, C.A., Shigue, C.Y., 2015. Study of Superconducting Fault Current Limiter Using Saturated Magnetic Core. J. Supercond. Nov. Magn. 28, 685–690. https://doi.org/10.1007/s10948-014-2871-y

Ferreira, F., Murta-Pina, J., Martins, J., 2015. Development of a computational tool for simulating inductive superconducting fault current limiters, in: 2015 9th International Conference on Compatibility and Power Electronics (CPE). Presented at the 2015 9th International Conference on Compatibility and Power Electronics (CPE), pp. 476–481. https://doi.org/10.1109/CPE.2015.7231122

Hasan, K.N., Rao, K.S.R., Mokhtar, Z., 2008. Analysis of load flow and short circuit studies of an offshore platform using ERACS software, in: 2008 IEEE 2nd International Power and Energy Conference. Presented at the 2008 IEEE 2nd International Power and Energy Conference, pp. 543–548. https://doi.org/10.1109/PECON.2008.4762535

Hekmati, A., 2014. Proposed Design for a Tunable Inductive Shield-Type SFCL. IEEE Trans. Appl. Supercond. 24, 1–7. https://doi.org/10.1109/TASC.2014.2311408

Hong, H., Cao, Z., Zhang, J., Hu, X., Wang, J., Niu, X., Tian, B., Wang, Y., Gong, W., Xin, Y., 2009. DC Magnetization System for a 35 kV/90 MVA Superconducting Saturated Iron-Core Fault Current Limiter. IEEE Trans. Appl. Supercond. 19, 1851–1854. https://doi.org/10.1109/TASC.2009.2019292

Morandi, A., Fabbri, M., Ribani, P.L., 2013. Coupled Electromagnetic-Thermal Model and Equivalent Circuit of a Magnetic Shield Type SFCL. IEEE Trans. Appl. Supercond. 23, 5602705–5602705. https://doi.org/10.1109/TASC.2013.2241383

Moriconi, F., De La Rosa, F., Darmann, F., Nelson, A., Masur, L., 2011. Development and Deployment of Saturated-Core Fault Current Limiters in Distribution and Transmission Substations. IEEE Trans. Appl. Supercond. 21, 1288–1293. https://doi.org/10.1109/TASC.2011.2104932

Neumueller, H.-W., Schmidt, W., Kraemer, H.-P., Otto, A., Maguire, J., Yuan, J., Folts, D., Romanosky, W., Gamble, B., Madura, D., Malozemoff, A.P., Lallouet, N., Ashworth, S.P., Willis, J.O., Ahmed, S., 2009. Development of Resistive Fault Current Limiters Based on YBCO Coated Conductors. IEEE Trans. Appl. Supercond. 19, 1950–1955. https://doi.org/10.1109/TASC.2009.2017902

Nikulshin, Y., Wolfus, Y., Friedman, A., Yeshurun, Y., Rozenshtein, V., Landwer, D., Garbi, U., 2016. Saturated Core Fault Current Limiters in a Live Grid. IEEE Trans. Appl. Supercond. 26, 1–4. https://doi.org/10.1109/TASC.2016.2524444

Qiu, D., Li, Z.Y., Gu, F., Huang, Z., Zhao, A., Hu, D., Wei, B.G., Huang, H., Hong, Z., Ryu, K., Jin, Z., 2018. Experiment study on an inductive superconducting fault current limiter using no-insulation coils. Phys. C Supercond. Its Appl. 546, 1–5. https://doi.org/10.1016/j.physc.2017.11.011

Rajabi, M., Mousavi G., S.M., 2019. Thermal performance improvement of magnetic-shield superconducting fault current Limiter, by using heat-sink in its structure. Phys. C Supercond. Its Appl. 556, 30–35. https://doi.org/10.1016/j.physc.2018.11.004

Raza, M., Peñalba, M.A., Gomis-Bellmunt, O., 2018. Short circuit analysis of an offshore AC network having multiple grid forming VSC-HVDC links. Int. J. Electr. Power Energy Syst. 102, 364–380. https://doi.org/10.1016/j.ijepes.2018.05.009

Santos, B.M.O., n.d. Simulação de Máquinas Supercondutoras de Fluxo Aprisionado com Fitas de Segunda Geração 115.

Sass, F., Sotelo, G.G., Junior, R. de A., Sirois, F., 2015. H-formulation for simulating levitation forces acting on HTS bulks and stacks of 2G coated conductors. Supercond. Sci. Technol. 28, 125012. https://doi.org/10.1088/0953-2048/28/12/125012

Vilhena, N., Arsénio, P., Murta-Pina, J., Pronto, A., Álvarez, A., 2015. A Methodology for Modeling and Simulation of Saturated Cores Fault Current Limiters. IEEE Trans. Appl. Supercond. 25, 1–4. https://doi.org/10.1109/TASC.2014.2374179

Wang, J.Z., Gong, W.Z., Xin, Y., Zhang, J.Y., Hu, X.M., Sun, Y.W., Wu, T.Q., Tian, B., Wang, Y., Hong, H., Niu, X.Y., Li, Q., Zhang, L.F., 2009. FEM simulations in designing saturated iron core superconducting fault current limiters, in: 2009 International Conference on Applied Superconductivity and Electromagnetic Devices. Presented at the 2009 International Conference on Applied Superconductivity and Electromagnetic Devices, pp. 52–55. https://doi.org/10.1109/ASEMD.2009.5306694

World Energy Outlook 2019 – Analysis [WWW Document], n.d. . IEA. URL https://www.iea.org/reports/world-energy-outlook-2019 (accessed 12.16.19).

Zhang, J.Y., Zi Qiang Wei, Hui Hong, Gong, W.Z., Xin, Y., 2011. Electromagnetic design of saturated iron core SFCL, in: 2011 International Conference on Applied Superconductivity and Electromagnetic Devices. Presented at the 2011 International Conference on Applied Superconductivity and Electromagnetic Devices, pp. 305–308. https://doi.org/10.1109/ASEMD.2011.6145129